Extremophiles (2019) 23:305–317
https://doi.org/10.1007/s00792-019-01082-y

ORIGINAL PAPER

Temperature adaptation of DNA ligases from psychrophilic organisms

Kristel Berg[1] · **Ingar Leiros**[1] · **Adele Williamson**[1]

Received: 4 December 2018 / Accepted: 15 February 2019 / Published online: 2 March 2019

Abstract
DNA ligases operating at low temperatures have potential advantages for use in biotechnological applications. For this reason, we have characterized the temperature optima and thermal stabilities of three minimal Lig E-type ATP-dependent DNA ligase originating from Gram-negative obligate psychrophilic bacteria. The three ligases, denoted Vib-Lig, Psy-Lig, and Par-Lig, show a remarkable range of thermal stabilities and optima, with the first bearing all the hallmarks of a genuinely cold-adapted enzyme, while the latter two have activity and stability profiles more typical of mesophilic proteins. A comparative approach based on sequence comparison and homology modeling indicates that the cold-adapted features of Vib-Lig may be ascribed to differences in surface charge rather than increased local or global flexibility which is consistent with the contemporary emerging paradigm of the physical basis of cold adaptation of enzymes.

Keywords ATP-dependent DNA ligase · Psychrophile · Enzyme activity · Temperature optima

Introduction

DNA ligases are DNA-joining enzymes essential for survival of all organisms, due to their critical roles in DNA replication and repair. Using ATP or NAD^+ as a cofactor, DNA ligases catalyze the formation of a phosphodiester bond between the 5′ phosphate of one DNA strand and the hydroxyl group at the 3′ end of the other DNA strand, producing an intact sugar–phosphate backbone. The enzymatic reaction mechanism can be divided into three nucleotidyl-transfer steps (Ellenberger and Tomkinson 2008); the first involves the activation of the enzyme through a nucleophilic attack by a lysine residue to the adenosine cofactor ATP or NAD^+, releasing nicotinamide mononucleotide for NAD-dependent ligases (NDLs) or di-phosphate in the case of ATP-dependent ligases (ADLs). Next, the nucleophilic 5′- phosphate of the DNA attacks the phosphoramide bond to form an adenylated-DNA intermediate. The final step involves attack of the 3′-nucleophilic hydroxyl group on the new pyrophosphate bond, forming a phosphodiester bond between the 5′ and 3′ positions of the DNA and releasing the AMP. All the three chemical steps depend on a divalent cation, which is usually Mg^{2+} or in some cases Mn^{2+}.

DNA ligases are divided into two main classes based on the cofactor required in step 1 of the enzymatic reaction. The ADLs use ATP and are found in all phylogenetic kingdoms, with eukaryotes, archaea, and many viruses possessing at least one ADL that is essential for DNA replication (by joining Okazaki fragments), and some encode multiple forms with dedicated roles in DNA repair (Ellenberger and Tomkinson 2008; Plocinski et al. 2017; Shuman and Glickman 2007). NDLs, meanwhile, are found almost exclusively in bacteria, where they function in both replication and repair (Dwivedi et al. 2008; Wilkinson et al. 2001). In the cases, where accessory ADLs are identified in bacteria, it is always in addition to the essential NDLs (Pitcher et al. 2007b).

Since the first X-ray crystal structure of an ADL was solved two decades ago from bacteriophage T7 (Subramanya et al. 1996), numerous structural analyses of bacterial, archaeal, and eukaryotic ADLs have followed (Nishida et al. 2006; Pascal et al. 2004, 2006; Kim et al. 2009; Petrova et al. 2012; Akey et al. 2006; Kaminski et al. 2018; Shi et al. 2018; Williamson et al. 2014, 2018), and the wide variety

Communicated by L. Huang.

Electronic supplementary material The online version of this article (https://doi.org/10.1007/s00792-019-01082-y) contains supplementary material, which is available to authorized users.

✉ Adele Williamson
adele.k.williamson@uit.no

[1] Present Address: Department of Chemistry, The University of Tromsø- The Arctic University of Norway, 9019 Tromsø, Norway

of domains and gene arrangements between the different classes of ligases has become evident. Crystallographic studies of bacteriophage T7 (Doherty and Wigley 1999; Subramanya et al. 1996) revealed a common core architecture of two essential catalytic core domains: the adenylation domain (AD) directly involved in catalysis and the site of step 1 enzyme adenylation and the smaller oligonucleotide/oligosaccharide binding domain (OB) that is also required for activity (Doherty and Suh 2000; Doherty and Wigley 1999). These core catalytic domains include six conserved motifs (I, III, IIIa, IV, V, and VI) which are involved in one or more steps of the ligation pathway (Shuman 2009). The AD and OB domains are connected by a flexible linker that allows them to reorient during DNA binding. An additional N-terminal DNA-binding domain has been described in the larger ADLs active in DNA replication in Eukarya and Archaea, and additional enzymatic domains with end-repair functions are appended to the large LigD enzymes involved in bacterial non-homologous end joining (Pitcher et al. 2007a). The Lig E group of ADLs, found predominantly in Gammaproteobacteria, do not use appending domains or unstructured loops for DNA binding or possess additional domains with independent enzymatic function; thus, these small ligases serve as a model for the minimal functional unit of the ATP-dependent ligases. The ADL from the marine psychrophile *Psychromonas* sp. strain SP041 (Psy-Lig) is the smallest DNA ligase that has been structurally studied, being 41 residues shorter than the minimal ChlV-Lig protein (Williamson et al. 2014). Recent structure–function analysis of Psy-Lig and the closely related Ame-Lig demonstrated a novel mode of ligase engagement with its DNA substrate that relies on well-ordered side-chain contacts on the surface of the conserved domains, rather than re-ordering of flexible loop regions to achieve encirclement of the DNA duplex as was previously observed for minimal viral ligases (Nair et al. 2007; Williamson et al. 2018). All Lig E-type ADLs have strong predictions for N-terminal leader sequences which are expected to direct them to the periplasm, and the demonstrated increase in activity and solubility when this predicted leader was not included in recombinantly produced *Aliivibrio salmonicida* (hereafter referred to as Vib-Lig) supports such signal processing (Williamson and Pedersen 2014). Although the biological role of such putatively periplasmic ligases and the source of ATP outside the cell remain to be determined, functions in competence and uptake of extracellular DNA have been proposed (Magnet and Blanchard 2004).

In the present study, we have characterized the temperature optima and thermal stability of Psy-Lig and Vib-Lig, both of which originate from obligate psychrophiles, along with a third homolog from *Pseudoalteromonas artica* (hereafter Par-Lig), isolated from sandy beach sediment on the Arctic island of Svalbard (Al Khudary et al. 2008). This builds on the previous work by Georlette et al. who conducted biophysical analyses and biochemical comparisons of larger, more complex NDLs from species spanning a range of growth temperature optima (Georlette et al. 2000; Georlette et al. 2003).

Living and thriving at low temperatures require that both enzyme kinetics and protein stability are adapted accordingly. It is now widely accepted that structural differences between cold-active enzymes and their mesophilic counterparts enable high specific activity at low temperatures, with a lower energy cost (D'Amico et al. 2002; Feller 2003; Struvay and Feller 2012). The physical origin of decreased temperature optima imparted by these structural changes is an active area of contemporary investigation (Åqvist et al. 2017; Arcus et al. 2016; Isaksen et al. 2016; Saavedra et al. 2018; van der Kamp et al. 2018), but it is generally observed that improved catalytic efficiency is accompanied by a reduced thermal stability and weaker substrate affinity, compared to thermophiles and mesophiles (Struvay and Feller 2012). For this reason, we have also carried out in silico comparisons of these Arctic-derived ADLs with mesophile-derived counterparts from human pathogens.

DNA ligases adapted to low temperatures offer novel potential advantages for use of these enzymes in biotechnological applications. Recently, the thermolability of a cold-adapted DNA ligase was used to develop a novel temperature-sensitive vaccine for tularemia (Duplantis et al. 2011), showing great potential in the biomedical sciences and other applications, where bacterial growth control is crucial. Furthermore, the enzymatic activity performed by DNA ligases in DNA replication and repair makes them useful tools in molecular biology and biotechnology applications, such as genetic engineering and next-generation DNA-sequencing technologies (Chambers and Patrick 2015; Shuman 2009; Tanabe et al. 2015). Cold-adapted enzymes have a potential advantage over mesophilic homologs by increasing yields of product at low temperatures, while suppressing contaminating nuclease activity. Finally, should the cold-active ligases be highly active, protocols may be carried out with smaller amounts of enzyme, due to better activity rates. In particular, short base-pair overhangs, i.e., 'sticky ends' generated by many restriction enzymes, will be stabilized due to the low melting temperature of short tracts of base-pairing involved. For these reasons, improving our understanding of temperature adaptation and identification of psychrophilic traits that could be used directly, or reverse-engineered into commercial ligase scaffolds has important biotechnological applications.

Methods

Protein expression and purification

ADLs from *Psychromonas* spp. strain SP041 (Psy-Lig) and *Aliivibrio salmonicida* (Vib-Lig) were expressed and

purified as described previously (Williamson and Pedersen 2014; Williamson et al. 2014). The gene encoding the Lig E-type ADL from *Pseudoalteromonas artica* (WP_010555135; Par-Lig), without the leader peptide, was synthesized by *Life Technologies* as the mature His-tagged, TEV-cleavable form with codon optimization for *E. coli* and supplied in the donor vector pDONR221. Transfer to the pHMGWA vector was done using Gateway® cloning (Thermo Fisher), and all steps including expression of the MBP fusion, purification, and tag removal were carried out as described for Psy-Lig and Vib-Lig.

Enzyme assays

Gel-based endpoint assays were carried out as described previously using 20 nt + 20 nt oligomers to form 40 nt product (Williamson et al. 2014, 2018). Details of substrate preparation are given in Table S1. Reactions contained 80 nM substrate, 1 mM ATP, 10 mM $MgCl_2$, 10 mM DTT, 50 mM NaCl, 50 mM Tris–HCl pH 8.0. Final enzyme concentrations of 2.5 µM and 100 µM were used for nicked and cohesive substrates, respectively. Enzymatic activity was detected by conversion of the FAM-labeled 20 nt substrate oligonucleotide into a 40 nt product, resolved by denaturing electrophoresis, detected by fluorescence on a Pharos FX Plus imager (Bio-Rad), and quantified by band intensity using the software Image J (Schneider et al. 2012). The extent of ligation activity was calculated from the ratio of these bands and expressed as a percentage. The temperature dependence of ligase activity was investigated by assaying for 15 min at temperatures between 5–55 °C for nicked substrates and 5–35 °C for cohesive substrates. Reactions were allowed to equilibrate for 1 min to the assay temperature, and then, the assay was started by addition of the enzyme.

Differential scanning calorimetry

Differential scanning calorimetry (DSC) experiments were carried out using an N-DSC III differential scanning calorimeter (Calorimetry Sciences Corporation). Purified ligases with concentrations of 1–2 mg ml^{-1} were extensively dialyzed against 50 mM HEPES pH 8.0, 100 mM NaCl to ensure complete equilibration. The enzymes were filtered through a 0.2 µm syringe filter (Millipore, Billerica, USA) and degassed for approximately 15 min before being loaded into the sample cell. The dialysis buffer was used as reference for baseline subtraction. Data analysis was performed using the program NanoAnalyse 2.4 (TA instruments). For each protein sample scanned, the corresponding buffer baseline was subtracted, and the data were normalized to the molar protein concentration calculated from the absorbance at 280 nm after dialysis and filtration. The calorimetric enthalpy was determined directly from the experimental data, and a theoretical two-state model was fitted using the routines provided in the program for determination of the van't Hoff enthalpy.

Thermofluor

Thermal denaturation of the purified ADLs with different buffers was examined by the thermofluor assay as described previously (Ericsson et al. 2006). Briefly, 5 µl of protein (1.0–1.5 mg ml^{-1}) was mixed with 1 µl of 300 × Sypro-Orange, 12.5 µl of 50 mM HEPES pH 8.0, 200 mM NaCl, added to the wells of a 96-well PCR plate (Bio-Rad) and sealed with Microseal® 'B' Adhesive Seals from Bio-Rad. Melting curves were recorded from 20 to 90 °C in increments of 0.3 °C per s using a MiniOpticon Real-Time PCR System with both FAM and HEX dye channels selected. T_m was determined using the supplied instrument software and monitoring the fluoresce of the HEX channel.

Sequence comparison

The amino acid sequences of Par-Lig, Psy-Lig, and Vib-Lig were aligned with the Lig E sequence from *Vibrio cholera* (Vch-Lig; gil147674166). N-terminal leader sequences were predicted using SignalP 4.1 and omitted from further analyses (http://www.cbs.dtu.dk/services/SignalP/) (Petersen et al. 2011). The ClustalW alignment tool in BioEdit was used to determine sequence identities and similarities. Conserved domains were analyzed by Pfam protein families' database at EMBL-EBI (http://pfam.xfam.org).

Homology modeling and analysis

Homology models of Vib-Lig, Par-Lig, and Vch-Lig were built based on the deposited crystal structure of Psy-Lig (4D05; (Williamson et al. 2014)). The sequences were uploaded to the Swiss-Model homology modeling server (Biasini et al. 2014). The A-chain of the deposited structure of Psy-Lig was selected as a modeling template for all modeled structure, as it has overall superior quality than the B-chain (with lower overall B-factor and amino acid residues generally better defined in electron density).

HBPLUS Hydrogen Bond Calculator v 3.2 (McDonald and Thornton 1994) was used to calculate hydrogen bonds in all PDB files. The hydrogen bonds included were those fulfilling the criteria for parameters donor (D), acceptor (A), acceptor antecedents (AA), and calculated hydrogen (H): maximum distance for D–A, 3.5 Å and H–A, 2.5 Å and minimum angle for D–H–A, D–A–AA, and H–A–AA of 90°. Ion-pair-interactions were investigated using the WHAT IF Web Interface (http://swift.cmbi.ru.nl/servers/html/index.html) (Vriend 1990), where interatomic distances between the side chains of the negatively charged Asp and Glu, and

the positively charges Arg, Lys, and His were tabulated with respect to being < 4 Å and < 6 Å. The APBS plugin in Pymol was used to estimate electrostatic surface potentials (Dolinsky et al. 2007).

Results

Temperature optimum and thermal stability

The aim of this study was to understand the determinants of low-temperature adaptation among DNA ligases. We chose to investigate the temperature optimum and thermal stability of Lig E ADLs from *Psychromonas* spp. strain SP041, *Aliivibrio salmonicida*, and *Pseudoalteromonas artica*, delineated Psy-Lig, Vib-Lig, and Par-Lig, respectively, as these represent psychrophilic species of bacteria isolated from a consistently low-temperature environments (Al Khudary et al. 2008; Egidius et al. 1986) (Table).

To analyze the temperature optima for ligase activity, gel-based endpoint assays were performed, both with single-nicked and overhanging substrates. Nick-sealing activity was measured by temperature intervals of 5 °C, ranging from 5 to 60 °C, or until the activity was abolished. For ligation of single-nicked substrates (Fig. 1a), there is a sharp peak of more than 50% ligation activity at around 20 °C for Vib-Lig, quickly declining to 10% activity at 30 °C, whereas the activity of Psy-Lig and Par-Lig increases with temperature from 15 °C up to an optimum of 35–40 °C, above which a sharp decline is observed. Although all ligases were cloned from psychrophilic organisms with similar growth temperatures, T_{opt} of their ligases for nicked substrates are different (Table 1).

The characterized ligases Psy-Lig, Par-Lig, and Vib-lig show a similar and relatively broad temperature optimum on the overhang substrate tested, with approximately 60–80% ligation activity from 5 to 25–30 °C, followed by a sharp decline at higher temperatures. As they all show better activity on overhang breaks at lower temperatures, we suggest that substrate stability rather than enzyme activity is the driving feature here. However, the enzymatic reaction will work very slowly at the low temperature, requiring a longer incubation time.

DSC experiments were performed to obtain a complete thermodynamic profile of the protein unfolding process of Psy-Lig, Par-Lig, and Vib-Lig. The melting temperature (T_m) was estimated to be significantly lower for Vib-Lig, 30.7 °C, compared to Psy-Lig and Par-Lig with T_m of 46.0 °C and 53.7 °C, respectively (Fig. 2a). All three ligases measured show a ratio > 1 between the van't Hoff enthalpy derived from fitting a two-state model, and the calorimetric enthalpy derived by integration of the area under the excess heat capacity curves. Such temperature profile indicates that

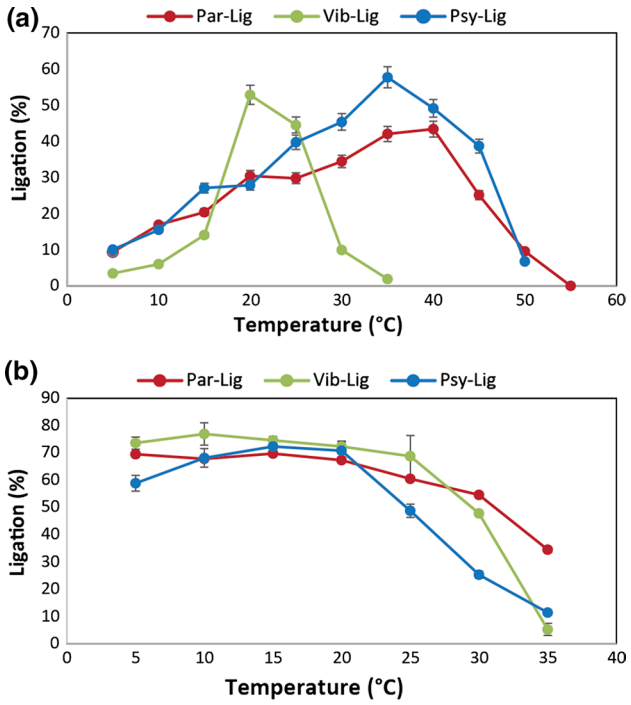

Fig. 1 Temperature optimum of Psy-Lig, Par-Lig, and Vib-lig by ligase activity assay. **a** Percentage of ligated single-nicked substrate. **b** Percentage of ligated cohesive substrate. Ligase activity was quenched after 15 min at various temperatures and quantified as percentage ligation by the intensity of the upper band relative to the sum of the two bands on the TBE-UREA gel. Ligase concentration was 2.5 µM for the nicked substrate and 100 µM for the cohesive substrate

Table 1 Literature and experimental data showing host optimal growth temperature, ligase temperature optimum for nick sealing and melting temperature

Ligase	Species of origin	Optimal growth (°C)	T_{opt} (°C)	T_m (°C)
Psy-Lig	*Psychromonas* spp. strain SP041	15[b]	35[a]	46[a]
Par-Lig	*Pseudoalteromonas artica*	10–15[c]	35–40[a]	53[a]
Vib-Lig	*Aliivibrio salmonicida*	15[d]	20[a]	30[a]

[a]This study

[b]Groudieva et al. (2003)

[c]Al Khudary et al. (2008)

[d]Egidius et al. (1986)

unfolding proceeds as a higher order oligomer; however, the irreversibility of the unfolding transition precluded detailed thermodynamic analysis.

The thermal stability in various buffer systems was measured by a thermofluor assay to confirm the DSC results and exclude the possibility that low thermal stability of observed for Vib-Lig is caused by non-ideal buffer conditions, as it

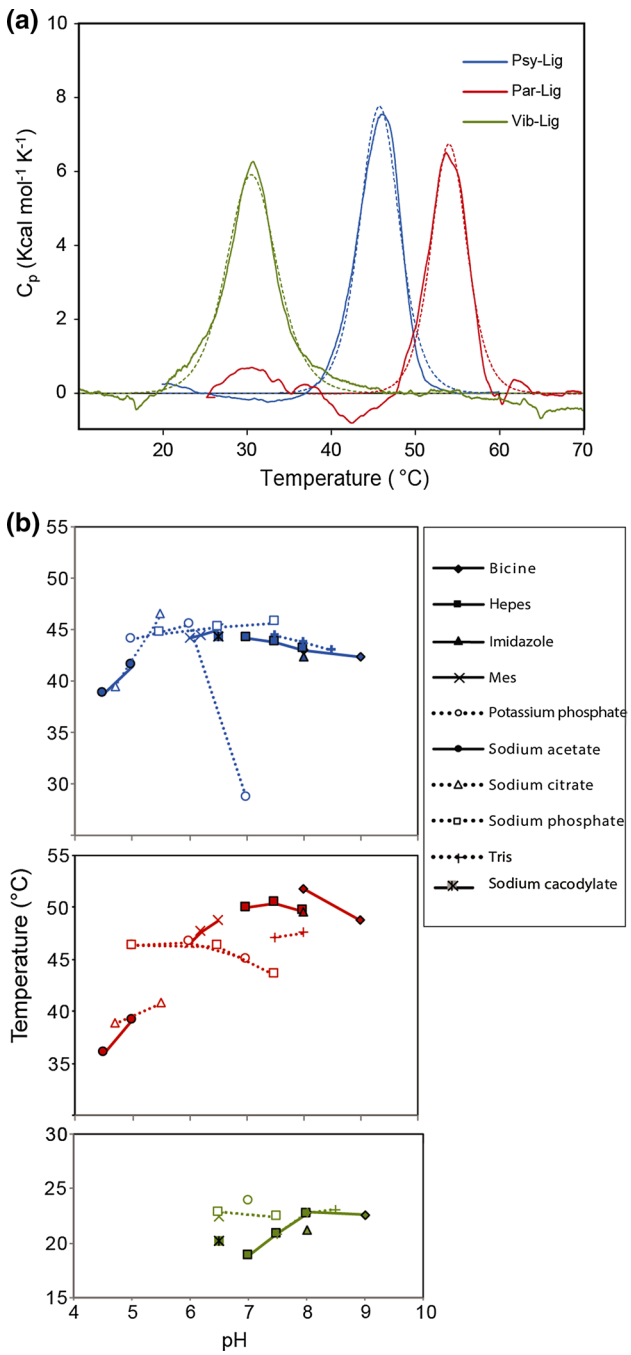

Fig. 2 Biophysical data. **a** Thermal unfolding monitored by DSC. **b** Thermal stability measured by thermofluor. Thermal unfolding parameters are given in Supplementary Table S2

has a significantly lower pI (predicted to be 5.5) relative to Psy-Lig and Par-Lig (both greater than 9.0). Thermofluor data (Fig. 2b) suggest that stability of the various ligases does not vary between pHs 6.5 and 9, with the exception of Psy-Lig which is extremely unstable in phosphate buffer at pH 7.0. Otherwise, Psy-Lig shows stability up to 46 °C and Par-Lig up to 53 °C, which is in line with DSC unfolding temperature. Also consistent with DSC data, Vib-Lig shows a lower thermal stability relative to Psy-Lig and Par-Lig with a maximum at 23 °C in all buffers down to pH 6.5. Below this, no transition could be observed, indicating that Vib-Lig was already unfolded.

Sequence comparison

Cold-active enzymes may combine rigidity and stability with a high level of flexibility. To gain further insight into the activity/stability/flexibility relationship and cold adaptation, interesting sequence and structural differences were identified by sequence alignments and homology modeling.

The enzymes studied are of similar size and share all properties common to minimal ADLs, but exhibit different temperature optima and stabilities. A structure-based sequence alignment was generated (Fig. 3). Lig E from *V. cholera* (Vch-Lig) was included as this human pathogen exhibits robust growth between 20 and 45 °C and is unable to survive at 4 °C for extended periods of time (Martinez et al. 2010). Pairwise comparison of the three experimentally examined Lig Es together with Vch-Lig shows that all sequence pairs have identities in the 40–49% range. Consistent with both enzymes deriving from members of the genus Vibrio, Vib-Lig and Vch-Lig share the highest homology in terms of sequence identity (48.4%), although they are adapted to different habitats and temperatures; thus, Vch-Lig represents a phylogenetically related mesophilic homolog of Vib-Lig. All four Lig Es contain the conserved nucleotidyltransferase family motifs I–VI and align with very few insertions or deletions, giving high confidence in placement of secondary structural elements by homology modeling (described below). Furthermore, the sequence alignment revealed high conservation of amino acids involved in substrate binding, metal binding and enzymatic activity.

Several studies have indicated the increased occurrence of some residues in cold-adapted proteins and decreased frequency of others, which has been rationalized by the physical properties of their sidechains influencing the flexibility and stability of the protein. This includes fewer salt bridges, fewer hydrogen bonds, a lower content of proline residues, a reduced Arg/(Arg + Lys) ratio, lower (Leu + Ile)/(Leu + Ile + Val) ratio and increased glycine content (Aghajari et al. 1998; Collins et al. 2005; Huston et al. 2004; Metpally and Reddy 2009; Russell et al. 1998; Saavedra et al. 2018). For this reason, we compared the amino acid content of the four proteins; however, most classic sequence 'traits' of cold adaptation, including increased glycine, decreased proline and less-packed hydrophobic core, were not apparent in Vib-Lig. Instead, higher sequence conservation appeared to be with the more phylogenetically related Vch-Lig than the other psychrophile-derived ADLs. For example, a lower number of Gly residues are often

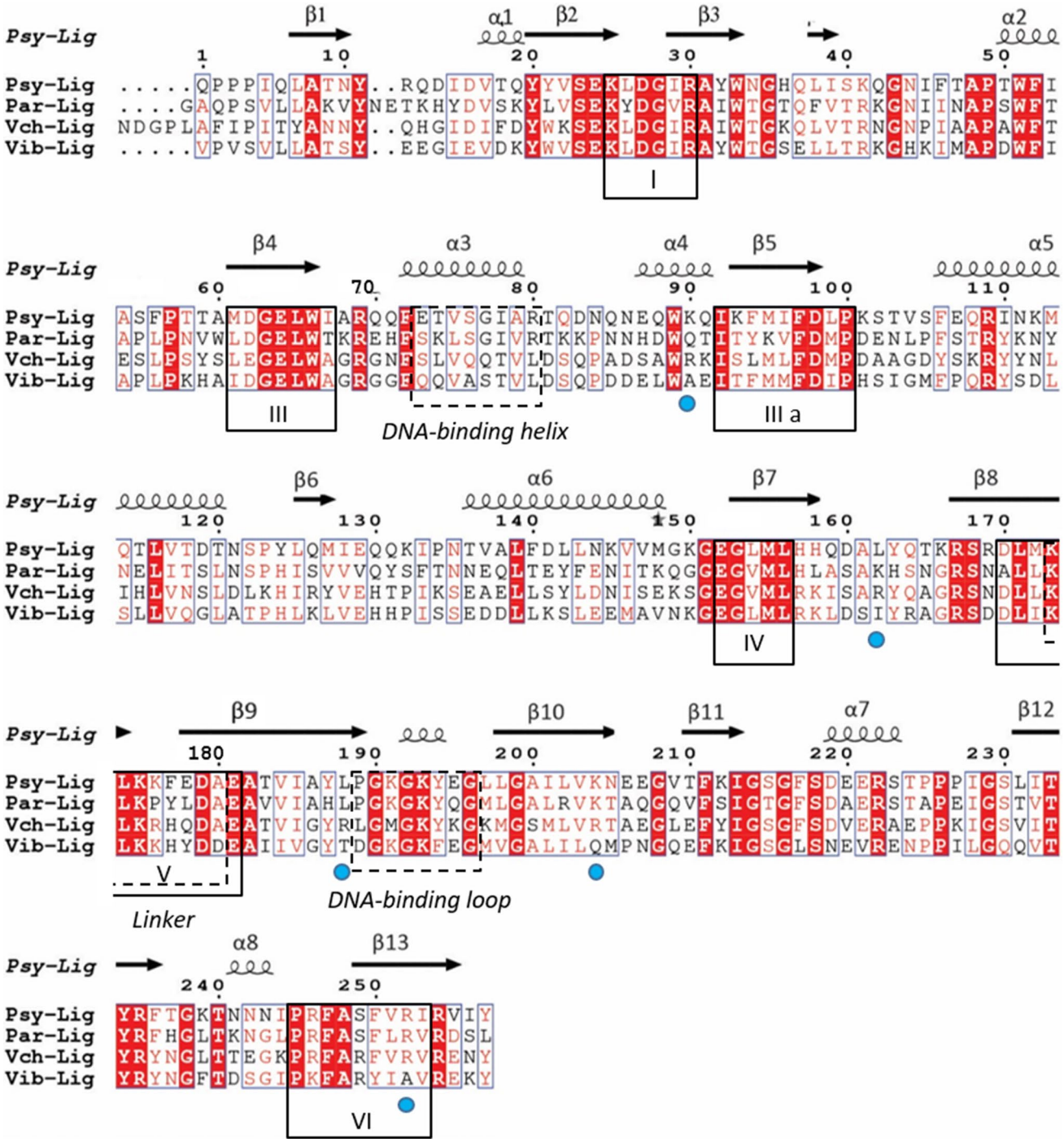

Fig. 3 Amino acid sequence alignment comparing mature ATP-dependent ligases from Psychromonas spp. strain SP041 (Psy-Lig), Aliivibrio salmonicida (Vib-Lig), Pseudoalteromonas artica (Par-Lig), and Vibrio cholera (Vch-Lig). Identical residues are shaded with red and similar residues are shown in red text. Spirals indicate α-helices and arrows indicate β-strands. Boxed amino acids represent conserved motifs of the nucleotidyltransferase enzymes. The DNA-binding elements of Lig Es are boxed with dashed lines. Surface-exposed substitutions of basic to uncharged residues in Vib-Lig are indicated by blue circles. Percentage sequence identity is given in Supplementary Table S3

pinpointed as a typical cold-adapted trait; however, this did not correlate with thermal stability of these ADLs, and most Gly residues are conserved, especially between the psychrophilic Vib-Lig and the mesophilic Vch-Lig (Table 2). Likewise, decreased Pro content has also been related to cold adaptation (Wallon et al. 1997; Zhao et al. 2010), but as Vch-Lig has fewer Pro than Vib-Lig (11 versus 13), Pro content is not an evident factor.

Another 'typical' feature of cold-adapted enzymes is a decreased number of Arg residues, which may increase stability through their capability to form hydrogen bonds and salt bridges (Aittaleb et al. 1997). In line with this, we observed the highest Arg count in the presumably mesophilic Vch-Lig (Table 2). The number of Arg residues is significantly lower for Vib-Lig (11), Psy-Lig (12), and Par-Lig (11) compared to Vch-Lig (18). This is also reflected by the ratio Arg/(Lys + Arg) per residue, which is 0.53 in Vch-Lig compared to 0.40, 0.39, and 0.39 in Psy-Lig, Vib-Lig, and Par-Lig, respectively, also supporting an overall better stability of the mesophilic molecule. Arg can contribute in more interactions with surrounding amino acids than lysine.

Table 2 Brief summary of extracted sequence features and characterization data for Psy-Lig, Vib-Lig, Par-Lig, and Vch-Lig, respectively

	Psy-Lig	Vib-Lig	Par-Lig	Vch-Lig
Sequence length	257	257	260	262
T_{opt} (°C)	35	20	35–40	–
T_{melt} (°C)	46.0	30.7	53.7	–
Calculated pI	9.1	5.3	9.5	9.0
Net charge[a]	+4	−9	+9	+4
Polar residues[b] (%)	35.8	29.2	37.3	34.0
Hydrophobic residues[c] (%)	41.3	42.8	39.2	39.7
Aromatic residues[d] (%)	10.9	9.7	11.2	11.5
Gly (number and %)	17/6.6	24/9.3	20/7.7	23/8.8
Met (number and %)	7/2.7	8/3.1	3/1.2	6/2.3
Pro (number and %)	13/5.1	13/5.1	12/4.6	11/4.2
Arg (number and %)	12/4.7	11/4.3	12/4.6	18/6.9
Arg/(Lys + Arg)	0.40	0.39	0.39	0.53
(Leu + Ile)/(Leu + Ile + Val)	0.76	0.70	0.65	0.78

[a]Residues R, K, D and E

[b]Residues G, S, T, Y, N, Q and C

[c]Residues A, V, L, I, W, F, P and M

[d]F, W and Y

However, Arg may also interact with water on the surface. Interestingly, the multiple sequence alignment (Fig. 3) shows that Arg in Vch-Lig is frequently substituted with hydrophobic residues in Vib-Lig.

Homology modeling and comparison to the crystal structure of Psy-Lig

To identify positions in the three-dimensional ligase structure, where relevant amino acid substitutions occurred, homology models of Par-Lig, Vib-Lig, and Vch-Lig were built based on the deposited structure of Psy-Lig 4D05; (Williamson et al. 2014). Increased local and/or global flexibility can be achieved by destabilization of the structure through a reduction in intramolecular forces such as salt bridges, ion-pair networks, hydrogen bonds and aromatic interaction, and increased length of loop regions (Davail et al. 1994; Feller 2003; Russell 2000). Hydrogen bond analysis shows that Vib-Lig is possibly destabilized by having fewer hydrogen bonds per residue in total, compared to Par-Lig and Psy-Lig (Table 3). In comparison, the mesophilic Vch-Lig has the highest ratio of hydrogen bonds per residue (0.816). It is interesting to note that the ratios correlate well with the measured melting temperatures Vib-Lig, Psy-Lig, and Par-Lig with low ratios giving low melting temperatures. In particular, the number of side-chain-to-main-chain hydrogen bonds is lower for the cold-adapted Vib-Lig.

Examination of the structural models also revealed that the arginine substitutions described in the preceding section are generally located on the surface, thus introducing hydrophobic surface patches in Vib-Lig (Fig. 4). Calculations by POPS (Parameter OPtimsed Surfaces (Fraternali and Cavallo 2002)) showed that the overall total area of exposed hydrophobic residues was similar among all ligases; thus, unique exposed hydrophobic patches in Vib-Lig appear to be local. Interesting Arg substitutions in Vib-Lig compared to Vch-Lig include Arg95–Ala90,

Table 3 Summary of calculated intramolecular interactions for Psy-Lig, Vib-Lig, Par-Lig, and Vch-Lig, respectively

	Psy-Lig	Vib-Lig	Par-Lig	Vch-Lig
PDB ID	4d05	Model	Model	Model
Resolution	1.65 Å	–	–	–
No. of residues in PDB file	257	256	257	250
No. of hydrogen bonds per residue	0.759	0.715	0.778	0.816
No. SS hydrogen bonds per residue	0.086	0.066	0.066	0.104
No. SM hydrogen bonds per residue	0.202	0.133	0.175	0.180
No. MM hydrogen bonds per residue	0.471	0.516	0.537	0.532
No. ion pairs < 4/< 6 Å	8/19	11/18	10/16	12/23
No. 2 membered networks < 4.0 Å	6	5	6	6
No. 3 membered networks < 4.0 Å	1	3	2	3

SS side-chain-to-side-chain hydrogen bonds, *SM* side-chain-to-main-chain hydrogen bonds, *MM* main-chain-to-main-chain hydrogen bonds

Arg167–Ile162, Arg193–Thr188, Arg209–Gln204, and Arg257–Ala252 (Fig. 4). For Par-Lig and Psy-Lig, three of these Arg are substituted with Leu/Lys. The percentage of hydrophobic residues is slightly higher for Vib-Lig (42.80%) and Psy-Lig (41.25%) compared to Par-Lig (39.25%) and Vch-Lig (39.69%), possibly reflecting the substitutions of polar residues with hydrophobic residues on the surface compared to Vch-Lig. In combination, the elevated number of hydrophobic residues described above, the unique local hydrophobic surface patches and the lower number of Arg, may impart local flexibility to the Vib-Lig structure compared to its mesophilic counterpart Vch-Lig.

Electrostatic surface potential

Some cold-adapted enzymes feature an overall excess of negative charges at the surface of the protein, with a pI frequently more acidic than that of their mesophilic homologues (Feller 2003; Leiros et al. 1999; Russell 2000). Higher frequency or patches of acidic residues on the surface may increase solvent interactions and thereby lead to an overall destabilization of the enzyme by charge–charge repulsion, observed in cold-adapted trypsin and β-lactamase (Feller 2003; Leiros et al. 1999). The calculated pI of 5.3 for Vib-Lig is significantly more acidic compared to its counterparts, and also correlates with the substitution of basic

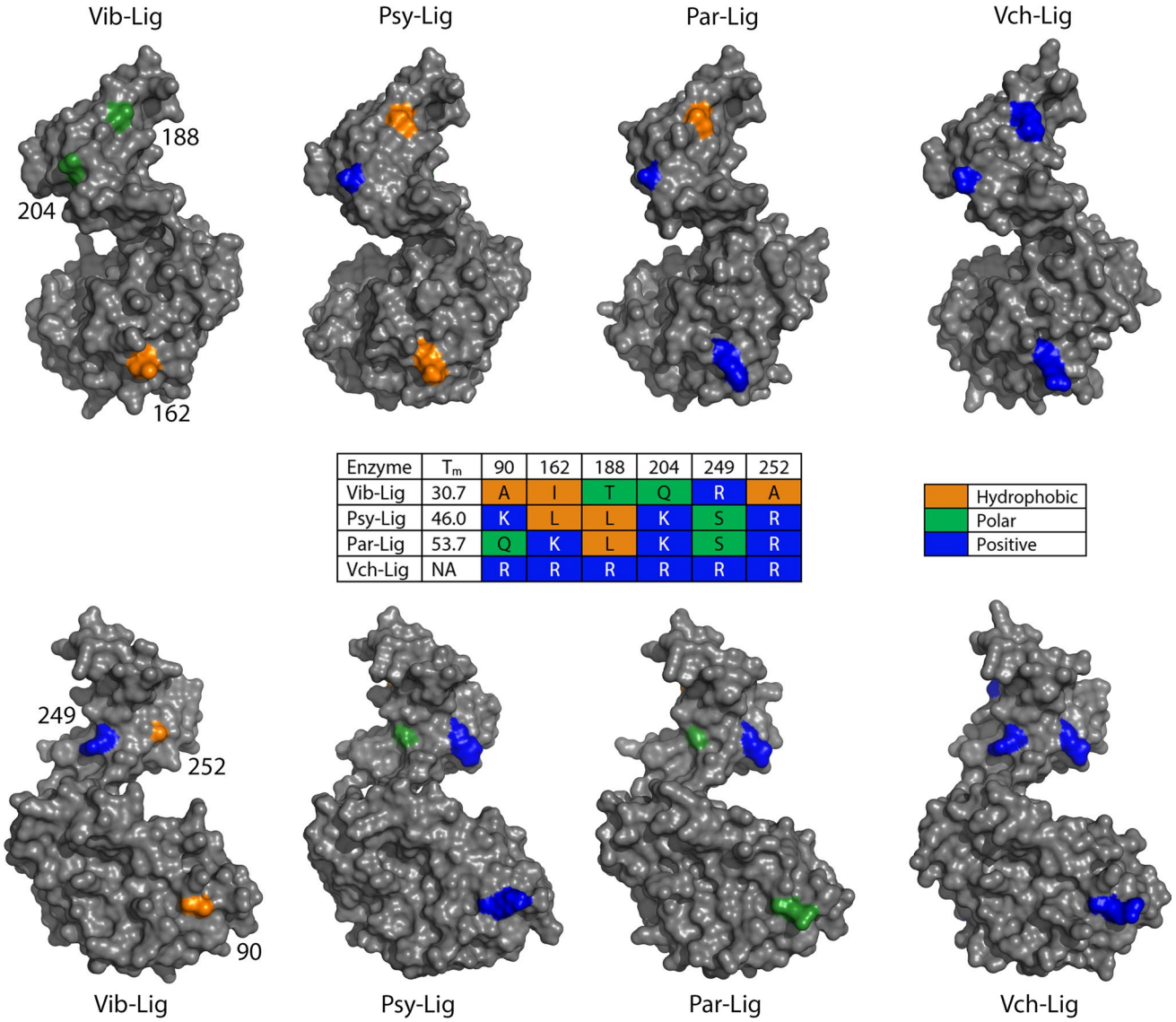

Enzyme	T_m	90	162	188	204	249	252
Vib-Lig	30.7	A	I	T	Q	R	A
Psy-Lig	46.0	K	L	L	K	S	R
Par-Lig	53.7	Q	K	L	K	S	R
Vch-Lig	NA	R	R	R	R	R	R

Fig. 4 Sequence variability mapped onto molecular surface representations of Vib-Lig, Psy-Lig, Par-Lig, and Vch-Lig. The top and bottom panels are rotated 180° views, while the middle panel shows melting temperature and substituted amino acids in selected positions for the four enzymes. Color codes: blue: positively charged residues; green: polar residues; orange: hydrophobic residues. Vib-Lig Residue numbers are included for reference between the panels

arginine residues at the surface with hydrophobic amino acids. Further examination of the charge distribution on the surface of the Vib-Lig model (Fig. 5) indicates that the DNA-binding faces of Vib-Lig remain positively charged as seen for structures of other Lig Es, while surfaces not involved in DNA binding are more positively charged compared with the more thermostable Psy-Lig. This suggests that charges in the binding surfaces of Vib-Lig are conserved and the majority of variation is located in distant areas of the protein.

Conservation of active site and DNA-binding surface

It is often suggested that low-temperature adaptation of enzymes is driven by increased local flexibility at the active site (D'Amico et al. 2002, 2006; Struvay and Feller 2012); therefore, we examined three key areas of the Vib-Lig enzyme that are essential for activity: the region surrounding the AMP-binding pocket, where the enzyme is covalently adenylated in the first step of the ligase reaction, the inter-domain linker region which undergoes significant structural changes during the catalytic cycle and the surfaces of the adenylation (AD-) and oligonucleotide-binding (OB-) domains that are in contact with double-strand DNA during nick sealing. Our comparisons reveal that the active site is strictly conserved, except for Lys 41 in Psy-Lig which is replaced by the chemically similar Arg in the other three ADLs (Fig. 3, supplementary Fig. S1a). The sequence alignment shows that the flexible linker regions connecting the two core domains are similar, preserving the hydrogen bonding pattern observed in Psy-Lig, with the exception of Par-Lig, where the equivalent of Lys 176 (Psy-Lig) is replaced by Pro (Fig. 3, supplementary Fig. S1b). Lig E-type ligases efficiently ligate DNA breaks without any additional DNA-binding domains or large flexible loop regions, instead using interactions with shorter highly structured motifs and specific charged residues found on the DNA-binding surface of the core catalytic domains (Williamson et al. 2014, 2018). In general, these motifs are well conserved between the three variants, consistent with both the equivalent positively charged DNA-binding surfaces of Vib-Lig and Psy-Lig and previous observations of consensus between Lig Es in this region (Fig. 5) (Williamson et al. 2018).

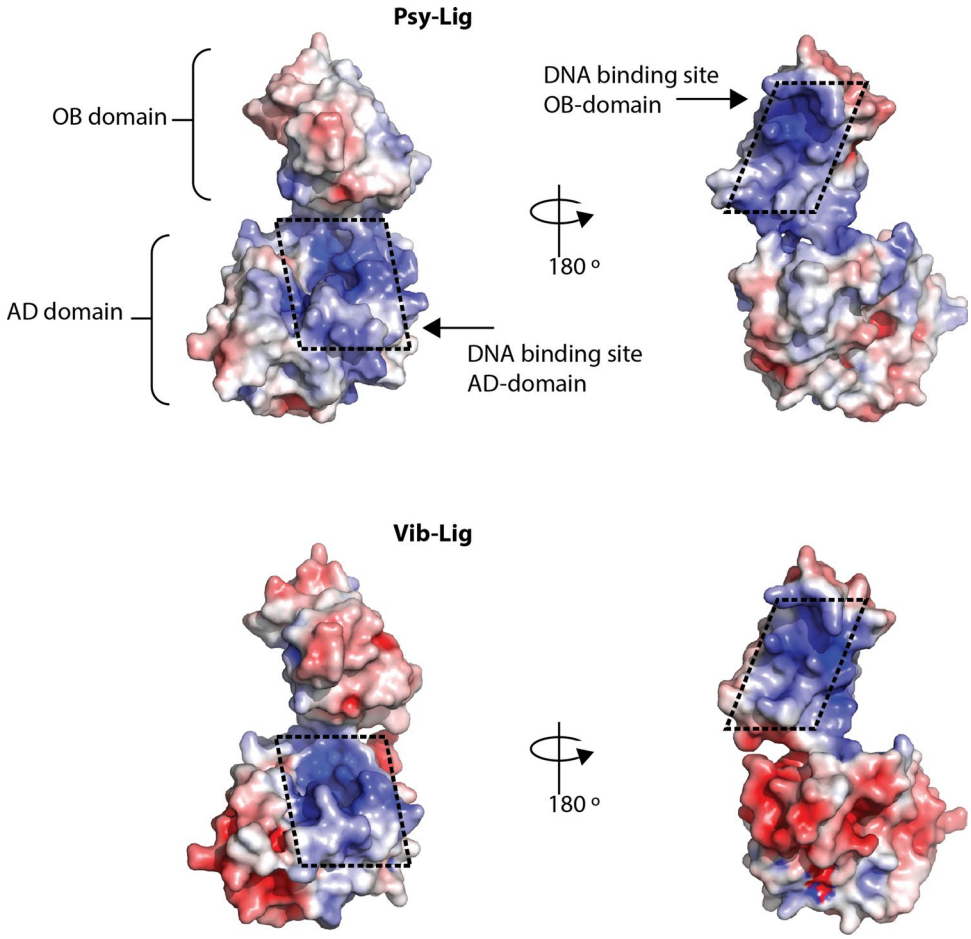

Fig. 5 Structure of Psy-Lig (top) and model of Vib-Lig (lower) colored surface charge. The surface potential was generated using APBS (Dolinsky et al. 2007), with positively charged areas shown in blue and negatively charged areas in red

Discussion

In this study, biochemical and biophysical characteristics of ATP-Dependent Ligases (ADLs) from psychrophilic organisms were analyzed in an attempt to identify typical cold-adaptation features. Vib-Lig, originating from the psychrophilic fish pathogen *Aliivibrio salmonicida* which has a growth range of 1–22 °C and an optimum of 15 °C (Egidius et al. 1986) exhibits classical features of cold adaptation including a low-temperature optimum of activity and decreased thermostability compared to homologous enzymes. In contrast, despite being derived from psychrophilic organisms, the Psy-Lig and Par-Lig enzymes are not themselves cold-adapted as both have temperature optima in the range of 35–40 °C and unfolding temperatures greater than 45 °C. This has been observed for many psychrophile-derived enzymes such as L-haloacid dehalogenase from *Psychromonas ingrahamii*, alcohol dehydrogenase of *Flavobacterium frigidimaris,* and KUC-12-keto acid decarboxylases derived from *Psychrobacter*, where the individual enzymes remain active and stable at temperatures well above the survival limit of the host organism (Kazuoka et al. 2007; Novak et al. 2013; Wei et al. 2013). The simplest rationale in the case of the ADLs is that although the temperature optimum is relatively high, the 30–40% activity recorded below 15 °C is sufficient for the biological purposes of the bacterium in its native environment, although the effects of different conditions on in vivo activity are also possible.

During ligation of double-strand breaks with cohesive ends, low temperature is an advantage to stabilize base-pairing between short stretches of complementary nucleotides at the break site. This must be balanced against decreased enzyme activity at lower temperatures. Lower temperatures allow DNA overhangs to base-pair and remain annealed long enough for the ligase to join them, at the expense of reduced ligase activity. This is directly observed in the present study during ligation of substrates with 4 nt overhangs as optimal activities are shifted to lower temperatures for all the three enzymes measured, despite of their individual T_{opt} varying when measured with a nicked substrate.

The Lig E enzymes compared in our study have moderate sequence identities (40–50%) and likely highly similar three-dimensional structures. The analyses performed indicated some sequence differences that potentially lower T_{opt} of Vib-Lig relative to homologs. One difficulty in such comparative analyses is distinguishing between substitutions imparting psychrophilicity and those that have occurred through genetic drift. To exclude possible false-positive findings based on phylogenetic resemblance, we included Lig E from *V. cholera* in our sequence comparison as previous phylogenomic studies have placed this close to Vib-Lig in evolutionary terms (Williamson et al. 2016), thus representing a genus-related but mesophilic organism. Coming from a mesophilic human pathogen, Vch-Lig is not anticipated to exhibit cold-adapted characteristics. The major differences in Vib-Lig appear to be in non-DNA-binding surface-exposed residues. Arginines are generally located on the surface of Psy-Lig, Par-Lig and Vch-Lig, and substitution of these residues introduces hydrophobic or uncharged surface patches in Vib-Lig. This is consistent with the investigation of three structurally homologous NAD^+-dependent DNA ligases (NDLs) adapted to different temperatures, where specific surface areas revealed a significant increase of exposed hydrophobic residues to solvent, in contrast to a more hydrophilic and charged surface area in thermophiles (Georlette et al. 2003), indicating an entropy-driven destabilization of the protein structure. Likewise, replacements of lysine with arginine in the psychrophilic α-amylase from *Pseudoalteromonas haloplanktis* resulted in a more stabilized enzyme with mesophilic properties, demonstrating the relevance of arginine content in cold adaptation (Siddiqui et al. 2006). It is interesting to note that these substitutions in Vib-Lig are unevenly distributed between the two domains with only two occurring in the larger catalytic adenylation domain (approximately 170 residues), and four on the smaller oligonucleotide domain (approximately 80 residues). Recent work demonstrated that substitutions increasing flexibility in different domains of adenylate kinase gave rise to different temperature effects on substrate binding and catalysis (Saavedra et al. 2018). As with DNA ligases, adenylate kinase activity involves coordinated reorientations between discrete protein domains, and it is interesting to consider whether this distribution reflects tuning of the oligonucleotide-binding domain for DNA binding/product release which are the rate limiting processes in the ligation reaction rather than the catalytic step its self (Bauer et al. 2017; Lohman et al. 2011).

Calculations of the electrostatic surface potential revealed that the cold-active Vib-Lig displays a positively charged surface near the active site and on the binding face of the OB-domain, which is important for binding of the negatively charged DNA substrate (Fig. 5), despite its overall more acidic pI. Similar results were observed for the cold-adapted uracil-DNA *N*-glycosylase (cUNG) from Atlantic cod (Leiros et al. 2003), indicating increased affinity for the negatively charged DNA compared with mesophile homologues. The number and nature of residues around the active site are conserved among the homologous ADLs adapted to different temperatures, suggesting that local cold-adapted residues are not directly involved in catalysis, but influence flexibility indirectly at some distance apart. The psychrophilic Vib-Lig is further

characterized by a decreased number of hydrogen bonds, which correlates with an increase in overall flexibility of the enzyme and affects protein-water surface interactions.

Although the decreased temperature optima of psychrophile-derived enzymes is commonly attributed to an increase in flexibility, either globally or locally, which causes a concomitant lowering of thermal stability (Smalas et al. 2000; D'Amico et al. 2002; Feller 2003; Struvay and Feller 2012), many enzymes are inactivated by temperatures below those inducing denaturation. A comparison of the NDL from the psychrophile *Pseudoalteromonas haloplanktis* with that of mesophilic NDL of *E. coli* and the thermophilic NDL of *Thermus scotoductus* indicated that structural differences imparted a temperature optimum of 18 °C, compared to 30 °C for NDL of *E. coli* and more than 60 °C for NDL of *T. scotoductus* (Georlette et al. 2000). This is accompanied by a decrease in T_m in the *P. haloplanktis* enzyme (33 °C) compared to the ones from *E. coli* (54 °C) and *T. scotoductus* (95–101 °C) (Georlette et al. 2003). The temperature optimum for activity of the *E. coli* NDL corresponds to the beginning of the thermal unfolding. *P. haloplanktis* NDL, however, shows a different link between activity and thermal adaptation; optimal activity is reached 10 °C before unfolding and the enzyme is inactivated at the beginning of the unfolding transition. A similar behaviour is observed for the activity and stability of Vib-Lig, Psy-Lig, and Par-Lig, where a decrease in activity above T_{opt} is observed in the absence of denaturation/unfolding. Recently, new paradigms have been suggested to explain this behaviour, as the classical (two-state) model is limited to enzymes, where increased catalytic activity is directly followed by thermal inactivation. These include macromolecular rate theory (MMRT), which provides a rationale for the curved temperature-rate plots observed for enzymes, independent of denaturation, and describes the temperature dependence of enzyme-catalyzed rates in the absence of denaturation by the difference in heat capacity between the enzyme–substrate complex and the enzyme transition state species (Arcus et al. 2016). The three-state equilibration model (EM) (Daniel and Danson 2013) has also been suggested to explain the temperature dependence of enzyme-catalyzed rates in the absence of denaturation. EM introduces a reversible inactivated (not denatured) form of the enzyme (E_{inact}) as an intermediate in rapid equilibrium with the active form (E_{act}), which adds a thermal buffer effect that protects the enzyme from thermal inactivation. Another explanation invokes a tuning of surface mobility through alteration of regions spatially removed from the active site which affect the overall enzyme dynamics (Åqvist et al. 2017; Isaksen et al. 2016). Computer simulations and Arrhenius plots suggest that surface rigidity/flexibility outside the catalytic region affects the enthalpy/entropy balance. Key single distant mutations may disrupt surface hydrogen bonding networks and alter the protein-water surface interactions (Isaksen et al. 2016) which may be the case with arginine substitutions in our study.

Conclusions

We have described the temperature optima and thermal denaturation profiles of three psychrophile-derived ADLs of the minimal Lig E-type. In the course of this work, we determined that two of the three, Par-Lig, and the structurally characterized Psy-Lig did not exhibit marked psychrophilic properties, while the third had typical low-temperature characteristics such as low T_{opt} and low thermal stability. Sequence comparison and homology modeling identified surface-exposed patches with greater hydrophobicity in Vib-Lig, relative to homologs, which we suggest are relevant for the experimentally observed psychrophilic properties.

Catalytic sites are often strictly conserved between homologs with different activity optima, as seen in Vib-Lig and Vch-Lig, meaning that the markedly lower T_{opt} of Vib-Lig relative to Psy-Lig and Par-Lig cannot be explained by increased active-site flexibility. We hope that future application of more sophisticated computational methods, coupled with specific mutational studies, may elucidate general principles imparting low-temperature activities. Such enhanced understanding of the molecular basis of low-temperature activity may enable us to tailor the activity optima of commercial ligases for use in biotechnological applications.

Acknowledgements This research was supported by Research Council Norway [244247, 2015]; Funding for open access charge was granted by the publication fund at the University of Tromsø.

References

Aghajari N, Feller G, Gerday C, Haser R (1998) Structures of the psychrophilic *Alteromonas haloplanctis* alpha-amylase give insights into cold adaptation at a molecular level. Structure 6:1503–1516

Aittaleb M, Hubner R, Lamotte-Brasseur J, Gerday C (1997) Cold adaptation parameters derived from cDNA sequencing and molecular modelling of elastase from Antarctic fish *Notothenia neglecta*. Protein Eng 10:475–477

Akey D, Martins A, Aniukwu J, Glickman MS, Shuman S, Berger JM (2006) Crystal structure and nonhomologous end-joining function of the ligase component of *Mycobacterium* DNA ligase D. J Biol Chem 281:13412–13423. https://doi.org/10.1074/jbc.M513550200

Al Khudary R, Stosser NI, Qoura F, Antranikian G (2008) *Pseudoalteromonas arctica* sp. nov., an aerobic, psychrotolerant, marine bacterium isolated from Spitzbergen. Int J Syst Evol Microbiol 58:2018–2024. https://doi.org/10.1099/ijs.0.64963-0

Åqvist J, Isaksen GV, Brandsdal BO (2017) Computation of enzyme cold adaptation. Nat Rev Chem 1:0051. https://doi.org/10.1038/s41570-017-0051

Arcus VL et al (2016) On the temperature dependence of enzyme-catalyzed rates. Biochemistry 55:1681–1688. https://doi.org/10.1021/acs.biochem.5b01094

Bauer RJ, Jurkiw TJ, Evans TC Jr, Lohman GJ (2017) Rapid time scale analysis of T4 DNA ligase-DNA binding. Biochemistry 56:1117–1129. https://doi.org/10.1021/acs.biochem.6b01261

Biasini M et al (2014) SWISS-MODEL: modelling protein tertiary and quaternary structure using evolutionary information. Nucleic Acids Res 42:W252–W258. https://doi.org/10.1093/nar/gku340

Chambers CR, Patrick WM (2015) Archaeal nucleic acid ligases and their potential in biotechnology. Archaea (Vancouver, BC) 2015:170571. https://doi.org/10.1155/2015/170571

Collins T, Gerday C, Feller G (2005) Xylanases, xylanase families and extremophilic xylanases. FEMS Microbiol Rev 29:3–23. https://doi.org/10.1016/j.femsre.2004.06.005

D'Amico S et al (2002) Molecular basis of cold adaptation. Philos T Roy Soc B 357:917–924. https://doi.org/10.1098/rstb.2002.1105

D'Amico S, Collins T, Marx JC, Feller G, Gerday C (2006) Psychrophilic microorganisms: challenges for life. EMBO Rep 7:385–389. https://doi.org/10.1038/sj.embor.7400662

Daniel RM, Danson MJ (2013) Temperature and the catalytic activity of enzymes: a fresh understanding. FEBS Lett 587:2738–2743. https://doi.org/10.1016/j.febslet.2013.06.027

Davail S, Feller G, Narinx E, Gerday C (1994) Cold adaptation of proteins. Purification, characterization, and sequence of the heat-labile subtilisin from the antarctic psychrophile *Bacillus*. TA41 J Biol Chem 269:17448–17453

Doherty AJ, Suh SW (2000) Structural and mechanistic conservation in DNA ligases. Nucleic Acids Res 28:4051–4058. https://doi.org/10.1093/nar/28.21.4051

Doherty AJ, Wigley DB (1999) Functional domains of an ATP-dependent DNA ligase. J Mol Biol 285:63–71. https://doi.org/10.1006/jmbi.1998.2301

Dolinsky TJ, Czodrowski P, Li H, Nielsen JE, Jensen JH, Klebe G, Baker NA (2007) PDB2PQR: expanding and upgrading automated preparation of biomolecular structures for molecular simulations. Nucleic Acids Res 35:W522–W525. https://doi.org/10.1093/nar/gkm276

Duplantis BN, Bosio CM, Nano FE (2011) Temperature-sensitive bacterial pathogens generated by the substitution of essential genes from cold-loving bacteria: potential use as live vaccines. J Mol Med JMM 89:437–444. https://doi.org/10.1007/s00109-010-0721-3

Dwivedi N, Dube D, Pandey J, Singh B, Kukshal V, Ramachandran R, Tripathi RP (2008) NAD(+)-dependent DNA ligase: a novel target waiting for the right inhibitor. Med Res Rev 28:545–568. https://doi.org/10.1002/med.20114

Egidius E, Wiik R, Andersen K, Hoff KA, Hjeltnes B (1986) *Vibrio salmonicida* sp. nov., a new fish pathogen. Int J Syst Evol Microbiol 36:518–520. https://doi.org/10.1099/00207713-36-4-518

Ellenberger T, Tomkinson AE (2008) Eukaryotic DNA ligases: structural and functional insights. Annu Rev Biochem 77:313–338. https://doi.org/10.1146/annurev.biochem.77.061306.123941

Ericsson UB, Hallberg BM, DeTitta GT, Dekker N, Nordlund P (2006) Thermofluor-based high-throughput stability optimization of proteins for structural studies. Anal Biochem 357:289–298. https://doi.org/10.1016/j.ab.2006.07.027

Feller G (2003) Molecular adaptations to cold in psychrophilic enzymes. Cell Mol Life Sci 60:648–662. https://doi.org/10.1007/s00018-003-2155-3

Fraternali F, Cavallo L (2002) Parameter optimized surfaces (POPS): analysis of key interactions and conformational changes in the ribosome. Nucleic Acids Res 30:2950–2960

Georlette D, Jonsson ZO, Van Petegem F, Chessa J, Van Beeumen J, Hubscher U, Gerday C (2000) A DNA ligase from the psychrophile *Pseudoalteromonas haloplanktis* gives insights into the adaptation of proteins to low temperatures. Eur J Biochem 267:3502–3512

Georlette D, Damien B, Blaise V, Depiereux E, Uversky VN, Gerday C, Feller G (2003) Structural and functional adaptations to extreme temperatures in psychrophilic, mesophilic, and thermophilic DNA ligases. J Biol Chem 278:37015–37023. https://doi.org/10.1074/jbc.M305142200

Groudieva T, Grote R, Antranikian G (2003) *Psychromonas arctica* sp. nov., a novel psychrotolerant, biofilm-forming bacterium isolated from Spitzbergen. Int J Syst Evol Microbiol 53:539–545. https://doi.org/10.1099/ijs.0.02182-0

Huston AL, Methe B, Deming JW (2004) Purification, characterization, and sequencing of an extracellular cold-active aminopeptidase produced by marine psychrophile *Colwellia psychrerythraea* strain 34H. Appl Environ Microbiol 70:3321–3328. https://doi.org/10.1128/aem.70.6.3321-3328.2004

Isaksen GV, Åqvist J, Brandsdal BO (2016) Enzyme surface rigidity tunes the temperature dependence of catalytic rates. Proc Natl Acad Sci 113:7822–7827. https://doi.org/10.1073/pnas.1605237113

Kaminski AM et al (2018) Structures of DNA-bound human ligase IV catalytic core reveal insights into substrate binding and catalysis. Nat Commun 9:2642. https://doi.org/10.1038/s41467-018-05024-8

Kazuoka T, Oikawa T, Muraoka I, Si Kuroda, Soda K (2007) A cold-active and thermostable alcohol dehydrogenase of a psychrotorelant from Antarctic seawater, *Flavobacterium frigidimaris* KUC-1. Extremophiles 11:257–267. https://doi.org/10.1007/s00792-006-0034-1

Kim DJ, Kim O, Kim HW, Kim HS, Lee SJ, Suh SW (2009) ATP-dependent DNA ligase from *Archaeoglobus fulgidus* displays a tightly closed conformation. Acta Crystallogr Sect F-Struct Biol Cryst Commun 65:544–550. https://doi.org/10.1107/s1744309109017485

Leiros HK, Willassen NP, Smalas AO (1999) Residue determinants and sequence analysis of cold-adapted trypsins. Extremophiles 3:205–219

Leiros I, Moe E, Lanes O, Smalas AO, Willassen NP (2003) The structure of uracil-DNA glycosylase from Atlantic cod (*Gadus morhua*) reveals cold-adaptation features. Acta Crystallogr D Biol Crystallogr 59:1357–1365

Lohman GJS, Chen LX, Evans TC (2011) Kinetic characterization of single strand break ligation in duplex DNA by T4 DNA ligase. J Biol Chem 286:44187–44196. https://doi.org/10.1074/jbc.M111.284992

Magnet S, Blanchard JS (2004) Mechanistic and kinetic study of the ATP-dependent DNA ligase of *Neisseria meningitidis*. Biochemistry 43:710–717. https://doi.org/10.1021/bi0355387

Martinez RM, Megli CJ, Taylor RK (2010) Growth and laboratory maintenance of *Vibrio cholerae*. Curr Protoc Microbiol 6:1. https://doi.org/10.1002/9780471729259.mc06a01s17

McDonald IK, Thornton JM (1994) Satisfying hydrogen bonding potential in proteins. J Mol Biol 238:777–793. https://doi.org/10.1006/jmbi.1994.1334

Metpally RP, Reddy BV (2009) Comparative proteome analysis of psychrophilic versus mesophilic bacterial species: insights into the molecular basis of cold adaptation of proteins. BMC Genom 10:11. https://doi.org/10.1186/1471-2164-10-11

Nair PA, Nandakumar J, Smith P, Odell M, Lima CD, Shuman S (2007) Structural basis for nick recognition by a minimal pluripotent DNA ligase. Nat Struct Mol Biol 14:770–778 http://www.nature.com/nsmb/journal/v14/n8/suppinfo/nsmb1266_S1.html

Nishida H, Kiyonari S, Ishino Y, Morikawa K (2006) The closed structure of an archaeal DNA ligase from Pyrococcus furiosus. J Mol Biol 360:956–967. https://doi.org/10.1016/j.jmb.2006.05.062

Novak HR, Sayer C, Panning J, Littlechild JA (2013) Characterisation of an L-haloacid dehalogenase from the marine psychrophile *Psychromonas ingrahamii* with potential industrial application. Mar Biotechnol (New York, NY) 15:695–705. https://doi.org/10.1007/s10126-013-9522-3

Pascal JM, O'Brien PJ, Tomkinson AE, Ellenberger T (2004) Human DNA ligase I completely encircles and partially unwinds nicked DNA. Nature 432:473–478. https://doi.org/10.1038/nature03082

Pascal JM et al (2006) A flexible interface between DNA ligase and PCNA supports conformational switching and efficient ligation of DNA. Mol Cell 24:279–291. https://doi.org/10.1016/j.molcel.2006.08.015

Petersen TN, Brunak S, von Heijne G, Nielsen H (2011) SignalP 4.0: discriminating signal peptides from transmembrane regions. Nat Meth 8:785–786 http://www.nature.com/nmeth/journal/v8/n10/abs/nmeth.1701.html#supplementary-information

Petrova T et al (2012) ATP-dependent DNA ligase from *Thermococcus* sp. 1519 displays a new arrangement of the OB-fold domain. Acta Crystallogr Sect F Struct Biol Cryst Commun 68:1440–1447. https://doi.org/10.1107/s1744309112043394

Pitcher RS, Brissett NC, Doherty AJ (2007a) Nonhomologous end-joining in bacteria: a microbial perspective. Annu Rev Microbiol 61:259–282. https://doi.org/10.1146/annurev.micro.61.080706.093354

Pitcher RS, Green AJ, Brzostek A, Korycka-Machala M, Dziadek J, Doherty AJ (2007b) NHEJ protects mycobacteria in stationary phase against the harmful effects of desiccation. DNA Repair. 6:1271–1276. https://doi.org/10.1016/j.dnarep.2007.02.009

Płociński P et al (2017) DNA Ligase C and Prim-PolC participate in base excision repair in mycobacteria. Nat Commun 8:1251. https://doi.org/10.1038/s41467-017-01365-y

Russell NJ (2000) Toward a molecular understanding of cold activity of enzymes from psychrophiles. Extremophiles 4:83–90. https://doi.org/10.1007/s007920050141

Russell RJ, Gerike U, Danson MJ, Hough DW, Taylor GL (1998) Structural adaptations of the cold-active citrate synthase from an Antarctic bacterium. Structure 6:351–361

Saavedra HG, Wrabl JO, Anderson JA, Li J, Hilser VJ (2018) Dynamic allostery can drive cold adaptation in enzymes. Nature 558:324–328. https://doi.org/10.1038/s41586-018-0183-2

Schneider CA, Rasband WS, Eliceiri KW (2012) NIH Image to ImageJ: 25 years of image analysis. Nat Meth 9:671–675

Shi K et al (2018) T4 DNA ligase structure reveals a prototypical ATP-dependent ligase with a unique mode of sliding clamp interaction. Nucleic Acids Res. https://doi.org/10.1093/nar/gky776

Shuman S (2009) DNA Ligases: progress and prospects. J Biol Chem 284:17365–17369. https://doi.org/10.1074/jbc.R900017200

Shuman S, Glickman MS (2007) Bacterial DNA repair by non-homologous end joining. Nat Rev Microbiol 5:852–861. https://doi.org/10.1038/nrmicro1768

Siddiqui KS et al (2006) Role of lysine versus arginine in enzyme cold-adaptation: modifying lysine to homo-arginine stabilizes the cold-adapted alpha-amylase from *Pseudoalteramonas haloplanktis*. Proteins 64:486–501

Smalas AO, Leiros HK, Os V, Willassen NP (2000) Cold adapted enzymes. Biotechnol Annu Rev 6:1–57

Struvay C, Feller G (2012) Optimization to low temperature activity in psychrophilic enzymes. Int J Mol Sci 13:11643–11665. https://doi.org/10.3390/ijms130911643

Subramanya HS, Doherty AJ, Ashford SR, Wigley DB (1996) Crystal structure of an ATP-dependent DNA ligase from bacteriophage T7. Cell 85:607–615

Tanabe M, Ishino Y, Nishida H (2015) From structure–function analyses to protein engineering for practical applications of DNA ligase. Archaea (Vancouver, BC) 2015:267570. https://doi.org/10.1155/2015/267570

van der Kamp MW, Prentice EJ, Kraakman KL, Connolly M, Mulholland AJ, Arcus VL (2018) Dynamical origins of heat capacity changes in enzyme-catalysed reactions. Nat Commun 9:1177. https://doi.org/10.1038/s41467-018-03597-y

Vriend G (1990) WHAT IF: a molecular modeling and drug design program. J Mol Graph 8(52–56):29

Wallon G et al (1997) Sequence and homology model of 3-isopropylmalate dehydrogenase from the psychrotrophic bacterium *Vibrio* sp. I5 suggest reasons for thermal instability. Protein Eng 10:665–672

Wei J, Timler JG, Knutson CM, Barney BM (2013) Branched-chain 2-keto acid decarboxylases derived from *Psychrobacter*. Fems Microbiol Lett 346:105–112. https://doi.org/10.1111/1574-6968.12208

Wilkinson A, Day J, Bowater R (2001) Bacterial DNA ligases. Mol Microbiol 40:1241–1248

Williamson A, Pedersen H (2014) Recombinant expression and purification of an ATP-dependent DNA ligase from *Aliivibrio salmonicida*. Protein Expres Purif 97:29–36. https://doi.org/10.1016/j.pep.2014.02.008

Williamson A, Rothweiler U, Schroder Leiros H-K (2014) Enzyme-adenylate structure of a bacterial ATP-dependent DNA ligase with a minimized DNA-binding surface. Acta Crystallogr Sect D 70:3043–3056. https://doi.org/10.1107/S1399004714021099

Williamson A, Hjerde E, Kahlke T (2016) Analysis of the distribution and evolution of the ATP-dependent DNA ligases of bacteria delineates a distinct phylogenetic group 'Lig E'. Mol Microbiol 99:274–290. https://doi.org/10.1111/mmi.13229

Williamson A, Grgic M, Leiros HS (2018) DNA binding with a minimal scaffold: structure–function analysis of Lig E DNA ligases. Nucleic Acids Res 46:8616–8629. https://doi.org/10.1093/nar/gky622

Zhao JS, Deng Y, Manno D, Hawari J (2010) *Shewanella* spp. genomic evolution for a cold marine lifestyle and in situ explosive biodegradation. PLoS One 5:9109. https://doi.org/10.1371/journal.pone.0009109